AMERICAN SOCIETY FOR MICROBIOLOGY | Journal of Virology®

STRUCTURE AND ASSEMBLY

The Ectodomain of the Vaccinia Virus Glycoprotein A34 Is Required for Cell Binding by Extracellular Virions and Contains a Large Region Capable of Interaction with Glycoprotein B5

Stephanie R. Monticelli,[a] Amalia K. Earley,[a]* Jessica Tate,[a]* Brian M. Ward[a]

[a]Department of Microbiology and Immunology, University of Rochester Medical Center, Rochester, New York, USA

ABSTRACT An interaction between the orthopoxvirus glycoproteins A34 and B5 has been reported. The transmembrane and ectodomain of A34 are sufficient for interaction with B5, localization of B5 to the site of intracellular wrapping, and subsequent incorporation into the envelope of released extracellular virions. Several mutagenic approaches were undertaken to better define the B5 interaction domain on A34. A set of C-terminal truncations in A34 identified residues 1 to 80 as sufficient for interaction with B5. Additional truncations identified residues 80 to 130 of A34 as sufficient for interaction with B5. To better understand the function of this region, a set of recombinant viruses expressing A34 with the full, partial, or no B5 interaction site (residues 1 to 130, 1 to 100, and 1 to 70, respectively) was constructed. All the recombinants expressing truncations of A34 incorporated B5 into extracellular virions but had a small-plaque phenotype similar to that of a virus with the A34R gene deleted (vΔA34R). Further characterization indicated that the small-plaque phenotype exhibited by these viruses is due to a combination of abrogated actin tail formation, reduced cell binding, and a defect in polyanion-induced nonfusogenic dissolution. Taken together, these results suggest that residues 80 to 130 of A34 are not necessary for the proper localization and incorporation of B5 into extracellular virions and, furthermore, that the C-terminal residues of A34 are involved in cell binding and dissolution.

IMPORTANCE Previous studies have shown that the vaccinia virus glycoproteins A34 and B5 interact, and in the absence of A34, B5 is mislocalized and not incorporated into extracellular virions. Here, using a transient-transfection assay, residues 80 to 130 of the ectodomain of A34 were determined to be sufficient for interaction with B5. Recombinant viruses expressing A34 with a full, partial, or no B5 interaction site were constructed and characterized. All of the A34 truncations interacted with B5 as predicted by the transient-transfection studies but had a small-plaque phenotype. Further analysis revealed that all of the recombinants incorporated detectable levels of B5 into released virions but were defective in cell binding and extracellular virion (EV) dissolution. This study is the first to directly demonstrate that A34 is involved in cell binding and implicate the ectodomain in this role.

KEYWORDS A34, B5, cell binding, glycoproteins, protein-protein interactions, vaccinia virus

Vaccinia virus (VACV), the prototypical member of the orthopoxviruses, was used as a live-attenuated virus vaccine for the eradication of variola virus, the causative agent of smallpox. VACV is a double-stranded DNA virus with a genome of approximately 200 kbp that carries approximately 200 open reading frames (ORFs) (1–3). Replication in the cytoplasm, at sites termed viral factories, results in multiple morphologically and antigenically distinct forms of the virus (4). Intracellular mature virus (IMV)

Citation Monticelli SR, Earley AK, Tate J, Ward BM. 2019. The ectodomain of the vaccinia virus glycoprotein A34 is required for cell binding by extracellular virions and contains a large region capable of interaction with glycoprotein B5. J Virol 93:e01343-18. https://doi.org/10.1128/JVI.01343-18.

Editor Rozanne M. Sandri-Goldin, University of California, Irvine

Copyright © 2019 American Society for Microbiology. All Rights Reserved.

Address correspondence to Brian M. Ward, Brian_Ward@urmc.rochester.edu.

* Present address: Amalia K. Earley, ACM Global, Rochester, New York, USA; Jessica Tate, Brammer Bio, Alachua, Florida, USA.

Received 16 August 2018
Accepted 12 November 2018
Accepted manuscript posted online 21 November 2018
Published 5 February 2019

is the first infectious form produced at the viral factory and contains a single lipid bilayer of unglycosylated viral proteins (5, 6). A small fraction of IMV is transported along the microtubule network to the intracellular site of wrapping, where it obtains an additional double-membrane envelope, derived from the virus-modified *trans*-Golgi network, producing intracellular enveloped virus (IEV) (7–10). IEV is subsequently transported to the cell periphery via microtubules, where the outermost membrane fuses with the plasma membrane to release double-membraned extracellular virions (EV) (11, 12). EV consist of either cell-associated enveloped virions (CEV), which remain associated with the surface of the cell and facilitate cell-to-cell spread via induction of actin tails (13), or extracellular enveloped virions (EEV), which are no longer attached to the cell surface and contribute to the long-range dissemination of the virus (14, 15).

At least nine VACV proteins, A33 (16), A34 (17), A36 (18), A56 (19), B5 (20), F12 (21), F13 (22), K2 (23), and E2 (24), are specific to IEV. Among these, A36 and F12 are not found on the released form, EV (18, 25). A56, A33, A34, B5, and K2 are exposed on the surface of EV and have been shown to be glycosylated (16, 17, 19, 26–28), whereas F13 is unglycosylated and found on the inner surface of the EV envelope (29). Specifically, recombinant viruses that have a deletion in any of these proteins, with the exception of A56 and K2, have a small-plaque phenotype, indicating a reduction in cell-to-cell spread (17, 20–22, 24). Interactions between B5 and A33 (30, 31), B5 and A34 (32, 33), A33 and A36 (32), A34 and A36 (33), B5 and F13 (34), F12 and E2 (35), F12 and A36 (36), and K2 and A56 (37) have been reported, with some of these interactions mediating intracellular trafficking and incorporation of EV proteins into IEV, IEV transport, and subsequent EV release.

Glycoprotein B5 is thought to play an important role in the intracellular wrapping of IEV to form EV, as deletion of this protein causes a reduction in the production of infectious EV (20, 38). B5 is a 42-kDa type I transmembrane glycoprotein consisting of a large extracellular domain/ectodomain (residues 1 to 275), a transmembrane domain (residues 276 to 303), and a short cytoplasmic tail (residues 304 to 317) (26). The ectodomain consists of four short consensus repeats and a predicted acidic stalk immediately adjacent to the transmembrane domain. Deletion of either the short consensus repeats or the cytoplasmic tail has no effect on EV formation (39, 40). A34 is a 19.6-kDa type II transmembrane glycoprotein with a C-type lectin-like domain (CTLD) (17). A single point mutation in the C terminus of A34, present in the VACV International Health Department J strain (IHD-J), causes a 50-fold increase in EEV release (41). Similarly, deletion of the A34R gene results in an increased release of EEV with a reduction in the specific infectivity of EV (42). Previously, we reported that A34 interacts with B5 and that this interaction is required for the localization of B5 to the site of IMV wrapping and subsequent incorporation into virion-sized particles (43).

Previous work mapped the interaction between A34 and B5 to the ectodomains of both proteins (33, 43). The present study focuses on further defining the region of A34 that interacts with B5 and examining the function of the interaction during infection. Using a transient-expression assay, residues 80 to 130 were determined to be sufficient for interaction with B5. Furthermore, we utilized the defined B5 interaction site to construct a set of recombinant viruses expressing either a full, partial, or no B5 interaction site to characterize the role of the A34-B5 interaction during infection. Our findings indicate that the B5 interaction site on A34 that we have defined here is not required for B5 localization to the site of wrapping or for incorporation into EV. However, these results indicate that the C-terminal residues of A34 play a role in actin tail formation, cell binding, and ligand-induced nonfusogenic dissolution.

RESULTS

The ectodomain of A34 is sufficient for interaction with B5. A34 is predicted to be a type II transmembrane protein with a small cytoplasmic domain (residues 1 to 17), a single transmembrane domain (residues 18 to 35), and an ectodomain (residues 36 to 168) that has similarities to CTLDs (17). Previous studies have shown that an A34 truncation containing only the predicted ectodomain and transmembrane domain

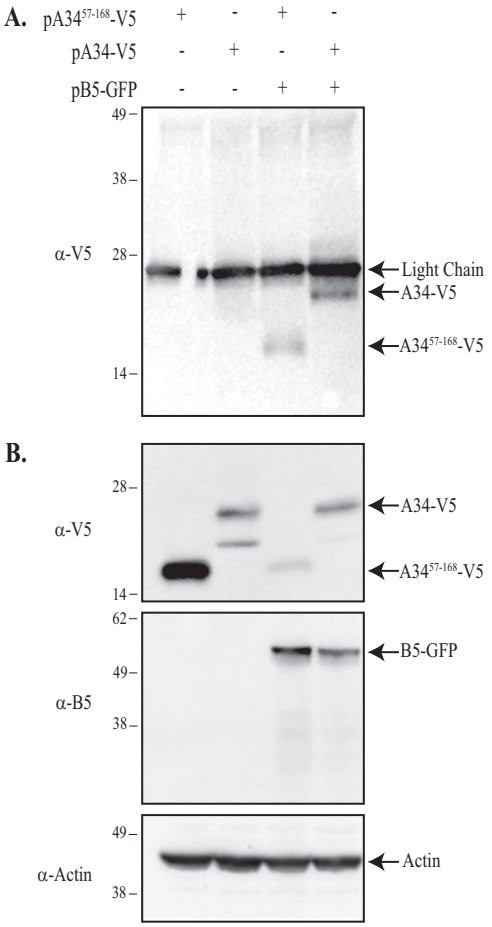

FIG 1 Coimmunoprecipitation of soluble A34. HeLa cells were infected with vTF7-3 at an MOI of 5 and transfected with the indicated plasmids in the presence of AraC. The following day, cells were lysed, and lysates were immunoprecipitated with anti-B5 and protein G-Dynabeads. Immune complexes (A) and cell lysates (B) were analyzed by Western blotting with anti-V5, anti-B5, and anti-actin. The masses in kilodaltons and positions of marker proteins are shown on the left of the blots.

was able to interact with B5-GFP (green fluorescent protein), whereas an A34 truncation containing the cytoplasmic and transmembrane domains could not (43). Furthermore, the ectodomain of B5 is sufficient for interaction with A34, suggesting that the corresponding B5 interaction domain on A34 is contained within the ectodomain (33, 43). To determine if the ectodomain of A34 alone is capable of interaction with B5, coimmunoprecipitation was performed with an A34 truncation that contained a cleavable signal sequence attached to the majority of the predicted ectodomain (pA34$^{57-168}$-V5) and full-length B5-GFP (Fig. 1A). Constructs were overexpressed in HeLa cells using the VACV T7 expression system in the presence of cytosine arabinoside (AraC) to block expression of postreplicative viral genes. The following day, cell lysates were immunoprecipitated with an anti-B5 antibody and processed for Western blotting (Fig. 1A). As had been seen previously, full-length A34 was immunoprecipitated by the anti-B5 antibody in the presence of B5-GFP (Fig. 1A). Importantly, the construct consisting of only the predicted ectodomain of A34 (A34$^{57-168}$-V5) was immunoprecipitated in the presence of B5-GFP (Fig. 1A). All of the constructs were expressed (Fig. 1B). Two forms of A34 were detected, with the slower-migrating band representing the fully glycosylated form and the faster-migrating band possibly containing an unglycosylated form of A34 (44, 45) (Fig. 1B). These data further substantiate the claim that the ectodomain of A34 is sufficient for interaction with B5.

Residues 1 to 80 of A34 are sufficient for interaction with B5. Previous results show that the ectodomain of A34 is sufficient for interaction with B5 (Fig. 1) (43). To

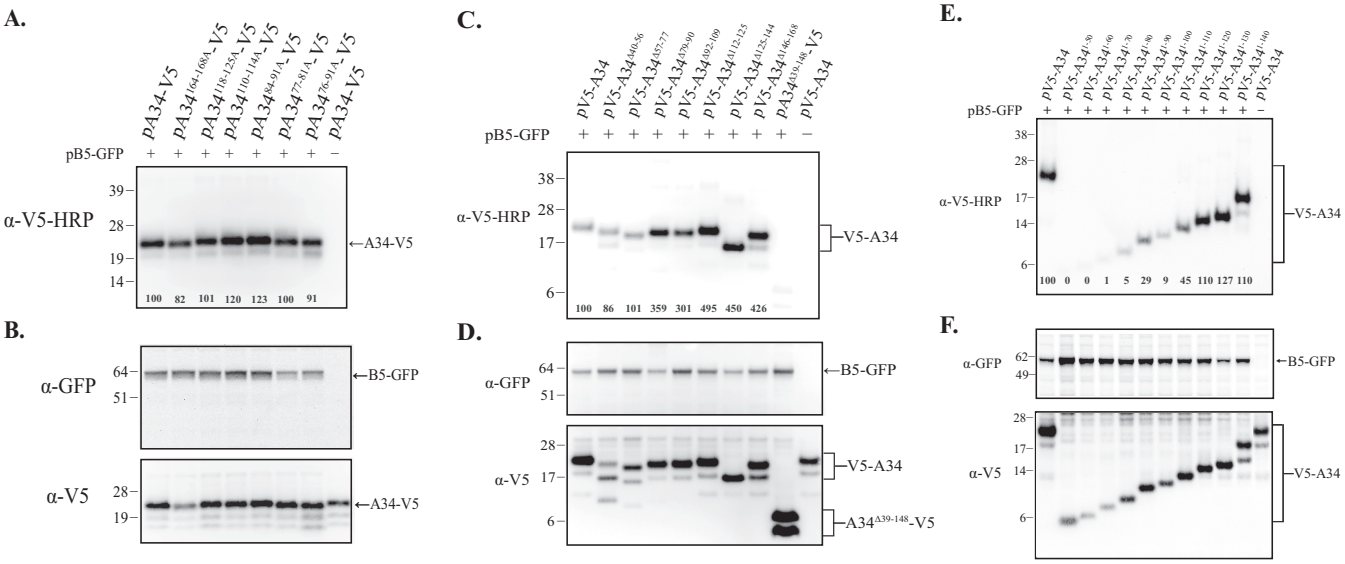

FIG 2 Coimmunoprecipitation of A34 mutation constructs. Shown is coimmunoprecipitation of A34 alanine mutation constructs (A and B) and internal (C and D) and C-terminal (E and F) deletion constructs. HeLa cells were infected with vTF7-3 at an MOI of 5 and transfected with the indicated plasmids in the presence of AraC. The following day, cells were lysed, and lysates were immunoprecipitated using an anti-B5 antibody. Immune complexes (A, C, and E) and cell lysates (B, D, and F) were analyzed by Western blotting with anti-V5 HRP-conjugated antibody, anti-GFP, and anti-V5 antibody. The masses in kilodaltons and positions of marker proteins are shown on the left of the blots. Bands were quantified, and percentages relative to A34-V5 or V5-A34 are presented.

further define residues in the ectodomain of A34 involved in the interaction with B5, several mutagenic approaches were tried. Most of the basic residues of A34 are clustered and contained within the ectodomain of A34, and it has been suggested that electrostatic forces between B5 and A34 are important for their interaction (46). For this reason, we created a panel of charge-to-alanine mutants in the ectodomain of A34. Charged residues in six of these clusters were mutated to alanine and had the V5 epitope tag appended to the C terminus. Constructs were overexpressed in HeLa cells using the VACV T7 expression system and tested for interaction with B5-GFP by coimmunoprecipitation using an anti-GFP antibody (Fig. 2A). However, all these mutants still coimmunoprecipitated with B5-GFP, indicating that the targeted mutations did not fully disrupt the B5-GFP/A34-V5 interaction (Fig. 2A). Western blot analysis of the cell lysates indicated that all of the A34 mutants were expressed (Fig. 2B).

As charge-to-alanine mutagenesis of the ectodomain of A34 failed to identify residues involved in the interaction with B5, we next created a series of small internal deletions in the ectodomain of A34 to try and target the B5 interaction domains. The deletions ranged in size from 12 to 20 residues and spanned the predicted ectodomain of A34. A total of 7 deletion mutants, each containing the V5 epitope tag at the N terminus, were put under the control of the T7 promoter and tested for interaction with B5-GFP by coimmunoprecipitation using an anti-B5 antibody (Fig. 2C). All of the A34 internal deletion mutants were expressed, and each one, with the exception of V5-A34$^{\Delta 125-144}$, produced multiple bands, which likely represent the different glycosylation states of A34 (Fig. 2D). As with the charge-to-alanine mutants, all the A34 internal deletion mutants still precipitated with B5-GFP, except for the complete A34 deletion, suggesting that by themselves, none of the deleted residues were sufficient to fully disrupt the interaction with B5.

As small mutations of A34 failed to determine the B5 interaction site (Fig. 2A to D), a more dramatic approach was taken by deleting increasingly larger segments of A34. A series of C-terminal truncations were made that sequentially removed 10 residues from the C terminus of A34. These constructs contained the cytoplasmic tail, the transmembrane domain, and the indicated number of residues in the ectodomain. The A34 truncation mutants were tested for interaction via coimmunoprecipitation as described above (Fig. 1). All the truncation mutants were expressed, as determined by

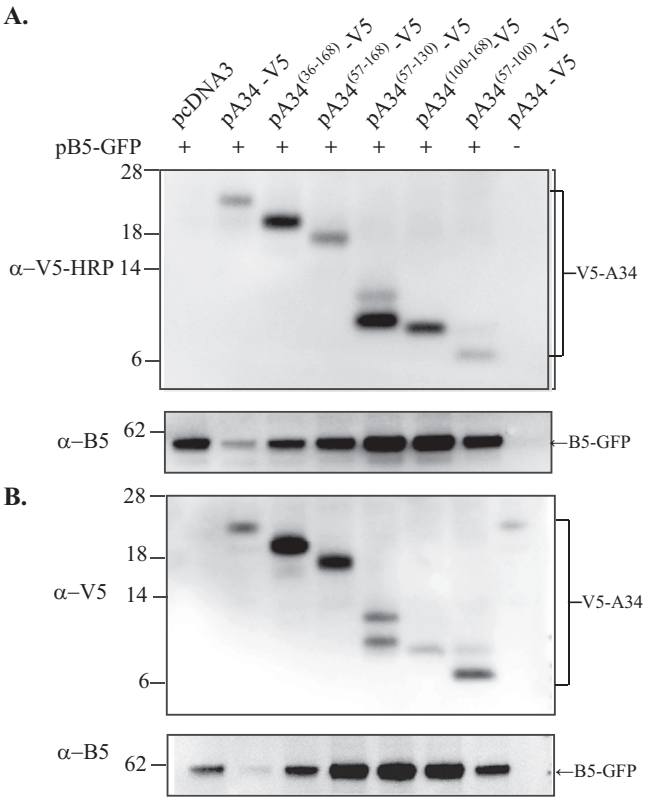

FIG 3 Coimmunoprecipitation of small regions of the A34 ectodomain. HeLa cells were infected with vTF7-3 at an MOI of 5 and transfected with the indicated plasmids in the presence of AraC. The following day, cells were lysed, and lysates were immunoprecipitated with anti-GFP and protein G-agarose. Immune complexes (A) and cell lysates (B) were analyzed by Western blotting with anti-V5-HRP, anti-B5, and anti-V5. The masses in kilodaltons and positions of marker proteins are shown on the left of the blots.

Western blot analysis (Fig. 2F), with lower expression levels for the constructs containing residues 1 to 60 and 1 to 70. A34 truncations that minimally included residues 1 to 80 of A34 coimmunoprecipitated with the anti-B5 antibody (Fig. 2E), whereas A34 truncations containing residues 1 to 70 or fewer of A34 were not readily detected (Fig. 2E). Although an interaction between B5-GFP and $A34^{1-80}$ was detected, it was noted that less $A34^{1-80}$ coimmunoprecipitated than for full-length A34. Only when residues 1 to 120 of A34 were present did levels similar to those of full-length A34 precipitate with B5-GFP, suggesting that residues 1 to 120 are necessary for a higher-affinity interaction with B5.

The ectodomain of A34 contains two separate regions capable of interaction with B5-GFP. We noticed that more B5 was precipitated with $A34^{1-120}$ than with $A34^{1-100}$, suggesting that there is a single large binding site for B5, for which a lower-affinity interaction occurs when residues 100 to 120 of A34 are absent. Alternatively, it is possible that A34 contains two separate binding sites for B5, one between residues 1 and 100 and another between residues 100 and 120. To determine the ability of this region to interact with B5, a second set of truncation mutants that contained small soluble regions of the ectodomain from A34 (residues 36 to 168, 57 to 168, and 57 to 130), or the two regions separately (residues 57 to 100, and 100 to 168), was generated. Each construct contained a cleavable signal sequence for translocation into the endoplasmic reticulum (ER) lumen and a C-terminal V5 tag. These constructs were put under the control of a T7 promoter and tested for interaction with B5-GFP by coimmunoprecipitation using an anti-GFP antibody (Fig. 3A). Constructs expressing residues 100 to 130 or 130 to 168 were created but failed to be expressed at detectable levels (Fig. 3B). As anticipated, the entire predicted ectodomain of A34 ($A34^{36-168}$-V5)

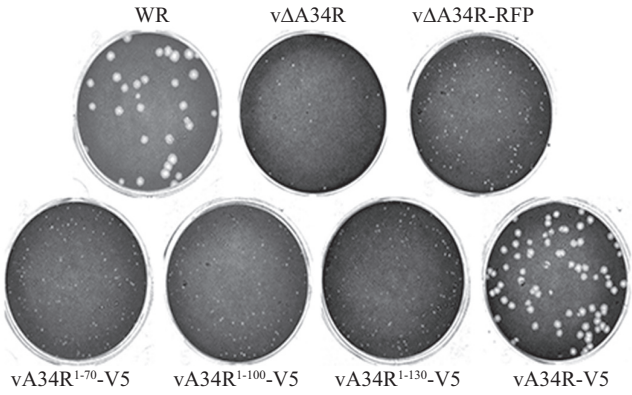

FIG 4 Plaque phenotype of recombinant A34R viruses. Monolayers of BSC-40 cells were infected with the indicated viruses and incubated at 37°C. After 2 h, the inoculum was removed, and cells were overlaid with semisolid medium. After 3 days at 37°C, the medium was removed, and cell monolayers were stained with crystal violet and imaged.

interacted with B5-GFP, as did the construct containing only residues 57 to 168 (Fig. 3A). Also, as predicted, both constructs containing residues 57 to 100 and 100 to 168 were sufficient for interaction with B5-GFP, demonstrating that, independently, these two regions (residues 57 to 100 and 100 to 168) are capable of interaction with B5 albeit to a lesser extent than the entire region as a whole. These data combined with the above-described data (Fig. 2) suggest that residues 80 to 130 of A34 likely encompass one large interaction site on A34 that contains two separate regions capable of interaction with B5.

Recombinant viruses containing C-terminal truncations in A34 confer a small-plaque phenotype. Our laboratory and others have shown that in the absence of A34, B5 is mislocalized and not incorporated into the envelope of released EV (33, 43). Furthermore, we have shown that A34 interacts with B5 through its ectodomain (Fig. 1) and hypothesized that the interaction is required for proper targeting and incorporation of B5 during infection. To examine the effect of this interaction on viral morphogenesis, we generated a set of recombinant viruses based on the B5 interaction site that we previously defined (Fig. 2 and 3). Each of the recombinant viruses expressed A34 containing a C-terminal V5 epitope tag and either a full (vA34R$^{1-130}$-V5), a partial (vA34R$^{1-100}$-V5), or no (vA34R$^{1-70}$-V5) B5 interaction site. Truncations were inserted into a virus that has red fluorescent protein (RFP) in the place of A34R (vΔA34R-RFP). To characterize these recombinants, we first examined the plaques produced by the mutants and compared them to plaques produced by the parent Western Reserve (WR) and a previously characterized virus that has A34R deleted (vΔA34R) (42). The plaque assay showed that vΔA34R-RFP had a plaque phenotype identical to that of vΔA34R (Fig. 4). When we replaced RFP with the entire coding sequence of A34R (vA34R-V5), the plaque phenotype was restored to that of WR, suggesting that A34R-V5 could functionally replace A34R. In contrast, each of the recombinants with truncations in A34 had a plaque phenotype similar to that of vΔA34R-RFP, regardless of whether the virus expressed A34 with or without the B5 interaction site (Fig. 4).

The altered A34-B5 interaction does not contribute to plaque size. The observation that each of the recombinants had a small-plaque phenotype (Fig. 4) suggested that the B5-A34 interaction during infection may differ from results obtained using the transient-transfection system (Fig. 2 and 3). To determine if the A34-B5 interaction is altered during infection, we examined the interaction in cells infected with our recombinants using coimmunoprecipitation. Consistent with our initial coimmunoprecipitations using the transient-overexpression system, a band corresponding to B5 was coimmunoprecipitated with A34 from lysates of cells infected with the recombinant virus expressing the full B5 interaction site (vA34R$^{1-130}$-V5) as well as vA34R-V5 (Fig. 5A). We also noticed that more B5 coimmunoprecipitated with vA34R$^{1-130}$-V5 than

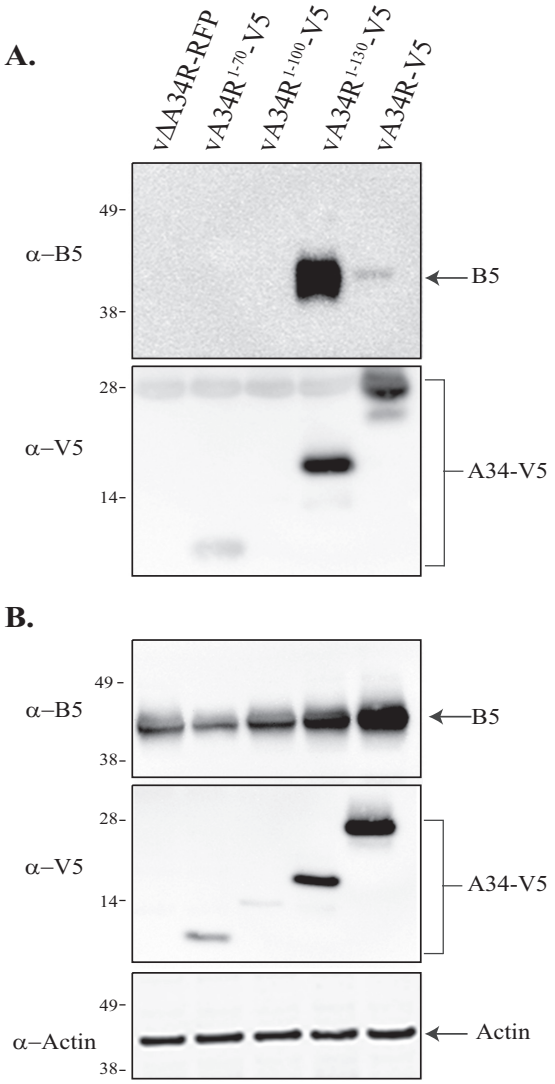

FIG 5 Coimmunoprecipitation of A34 from infected cells. HeLa cells were infected with the indicated viruses at an MOI of 5. The following day, cells were lysed, and lysates were immunoprecipitated with anti-V5 and protein G-Dynabeads. Immune complexes (A) and cell lysates (B) were analyzed by Western blotting with anti-V5, anti-B5 antiserum, and anti-actin. The masses in kilodaltons and positions of marker proteins are shown on the left of the blots.

with full-length A34 (Fig. 5A). We theorized that B5 was interacting with A34 in cells infected with the recombinant expressing the partial B5 interaction site (vA34R$^{1-100}$-V5), but we were not able to detect this interaction due to poor expression of the truncation (Fig. 5B). As expected, we were unable to detect a band corresponding to B5 upon V5 coimmunoprecipitation either in lysates of cells infected with the recombinant virus missing the B5 interaction site (vA34R$^{1-70}$-V5) or from the recombinant virus lacking A34R (vΔA34R-RFP) (Fig. 5A). These data indicate that the small-plaque phenotype for A34R$^{1-130}$-V5 is not due to an altered B5 interaction with residues 80 to 130 of A34.

B5 localizes to the site of wrapping in the absence of residues 80 to 130 of A34. Previous reports have shown that in the absence of A34, the majority of B5 fails to localize to the site of wrapping (43), suggesting that the A34-B5 interaction is required for localization of B5 to the site of wrapping. To understand if B5 mislocalization was an underlying cause of the small-plaque phenotype, we examined the intracellular localization of B5 and A34. Cells on coverslips were infected with the recombinant viruses and subsequently fixed, permeabilized, and stained with anti-B5 and anti-V5

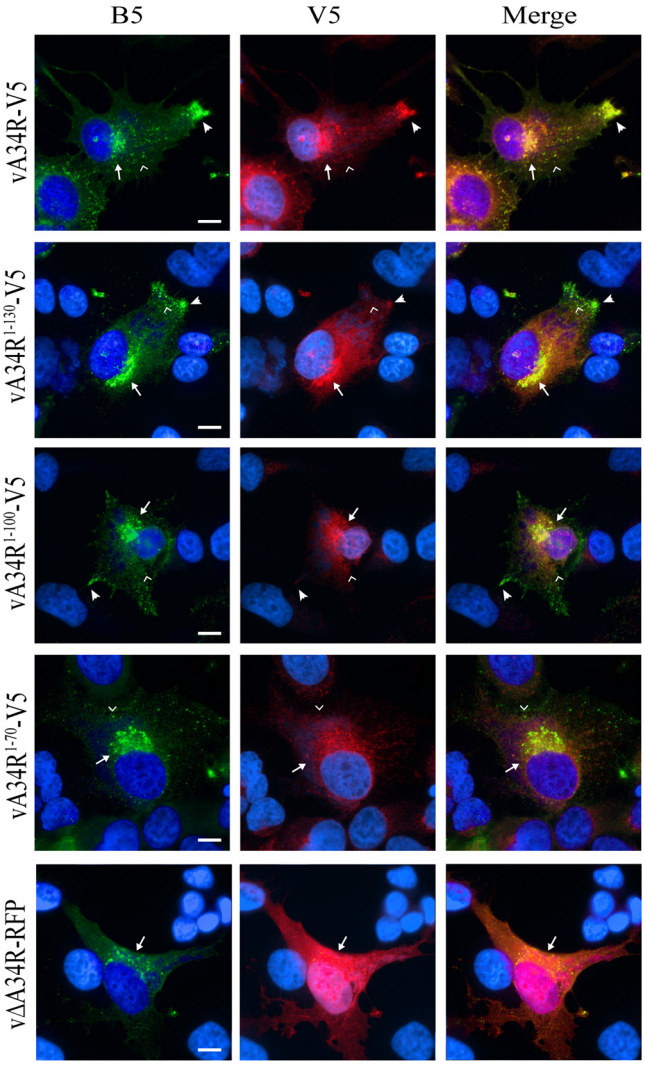

FIG 6 Intracellular localization of B5 and A34. HeLa cells were grown on coverslips and infected with the indicated viruses at an MOI of 0.5. The next day, cells were fixed, permeabilized, and incubated with anti-B5 and anti-V5 mAbs followed by Cy2-conjugated anti-rat (green) and Alexa Fluor 594-conjugated anti-mouse (red) antibodies. Coverslips were mounted on microscope slides with ProLong Gold antifade reagent with DAPI to stain DNA-containing particles (blue) and imaged via fluorescence microscopy. The overlap of B5 (green) and V5 (red) is shown in yellow. Localization at the site of wrapping, at the cell vertices, and at VSPs is represented by arrows, concave arrowheads, and arrowheads, respectively. Red staining in the vΔA34R-RFP panel refers to RFP fluorescence and not V5 staining. Bars, 10 μm.

(Fig. 6). We compared the localization of B5 and A34 in cells infected with the recombinant viruses expressing C-terminal truncations in A34 to that in cells infected with vA34R-V5 and vΔA34R-RFP. Cells infected with vA34R-V5 showed that B5 and A34 colocalize to the site of wrapping (Fig. 6, arrows), at the cell vertices (Fig. 6, concave arrowheads), and in virion-sized particles (VSPs) (Fig. 6, arrowheads). However, during infection with vΔA34R-RFP, B5 staining was absent from the cell vertices, few to no B5-stained VSPs were detected, and B5 staining at the site of wrapping was reduced. For the viruses expressing the full and partial B5 interaction sites (vA34R$^{1-130}$-V5 and vA34R$^{1-100}$-V5, respectively), B5 was localized similarly to vA34R-V5, with B5 staining at the site of wrapping, at the cell vertices, and in VSPs. However, A34 localization was more diffuse throughout the cell, giving a lacy fluorescence pattern, and was mostly absent from VSPs compared to cells infected with vA34R-V5, although A34 was still concentrated at the site of wrapping and colocalized with B5 at this location. In cells infected with the virus lacking the B5 interaction site (vA34R$^{1-70}$-V5), B5 and A34

localization to the site of wrapping was less defined, and B5 was completely absent from the cell vertices, although there were still B5-labeled VSPs. Altogether, these data suggest that B5 is properly localized in cells infected with our recombinant viruses, despite the presence or absence of the defined B5 interaction site (residues 80 to 130) on A34.

Actin tail production is abrogated by removal of the A34 C terminus. During infection, CEV induce actin tail formation at the plasma membrane to propel CEV away from the cell surface of infected cells, increasing cell-to-cell spread of the virus (13). Furthermore, previous work has shown that actin tail production contributes to plaque size (15, 47). To determine if our recombinant viruses were capable of producing actin tails, we stained cells infected with our recombinant viruses for filamentous actin (F-actin). Unpermeabilized cells infected with vA34R-V5, vA34R$^{1-130}$-V5, vA34R$^{1-100}$-V5, vA34R$^{1-70}$-V5, or vΔA34R-RFP were immunostained for B5 to visualize CEV and subsequently permeabilized and stained with phalloidin-Alexa Fluor 647 to visualize F-actin. On the surface of cells infected with vA34R-V5, numerous actin tails tipped with B5-labeled VSPs were readily observed (Fig. 7). Notably, the site of wrapping was not stained, confirming that cells were not permeabilized prior to actin staining. As was previously reported, actin tails were not detected on the surface of cells infected with vΔA34R-RFP (33, 48). Although B5-labeled VSPs were present on the surface of cells infected with each of the recombinants, with the exception of vΔA34R-RFP, actin tails underneath these B5-labeled VSPs were not observed for the recombinant viruses expressing A34 truncations, suggesting that actin tail formation is abrogated by removal of the C-terminal residues of A34.

B5- and A34-labeled VSPs are present on the surface of cells infected with recombinant viruses. The presence of B5-stained VSPs suggested that B5 was incorporated into virions (Fig. 6 and 7); therefore, we next wanted to determine if the B5-stained VSPs on the cell surface also contained the C-terminal truncations of A34. Cells on coverslips were infected with the recombinant viruses and subsequently fixed and stained with anti-B5 and anti-V5 monoclonal antibodies (mAbs) without permeabilization (Fig. 8). Cells infected with vA34R-V5 showed colocalization of A34 and B5 in VSPs (Fig. 8, arrowheads); however, during infection with vΔA34R-RFP, few to no B5-stained VSPs were present (Fig. 8), and B5 was predominantly present on the plasma membrane. Similarly to vA34R-V5 staining, A34 and B5 colocalized to VSPs in cells infected with our recombinant viruses expressing C-terminal truncations in A34 (Fig. 8). Importantly, the site of wrapping was not stained by either B5 or V5, indicating that the infected cells were not permeabilized. In addition, there appeared to brighter staining of the plasma membrane in these cells (Fig. 8) than in the permeabilized samples (Fig. 6) due to the absence of detergent during processing. Altogether, these data suggested that both B5 and A34 are incorporated into EV for each of our recombinants and, furthermore, that the B5 interaction site described here (residues 80 to 130 of A34) is not necessary for the incorporation of B5.

Deletion of the C-terminal residues of A34 results in a reduction of B5 and A33 incorporation into EEV. Previous reports indicated that an interaction with A34 would be required for the incorporation of B5 into EV. Therefore, we initially hypothesized that residues 80 to 130 of A34 would be required for B5 incorporation. However, our immunofluorescence data suggested that B5 is properly localized to the site of wrapping and incorporated into VSPs, even for recombinants with a missing or partial B5 interaction site (Fig. 6 to 8). To determine if B5 and truncated A34 are incorporated into the envelope of EV produced from these recombinant viruses, EV in the supernatant was purified from cells infected with the recombinant viruses and assayed for B5, A33, and A34 via Western blotting (Fig. 9A). A band of a similar intensity corresponding to B5 was present in lysates from EV for vA34R$^{1-130}$-V5, vA34R$^{1-100}$-V5, and vA34R$^{1-70}$-V5 albeit at reduced levels compared to vA34R-V5, suggesting that residues 80 to 130 of A34 are not required for B5 incorporation and confirming our immunofluorescence results (Fig. 9A). Furthermore, even less B5 was detected in EV produced from vΔA34R-

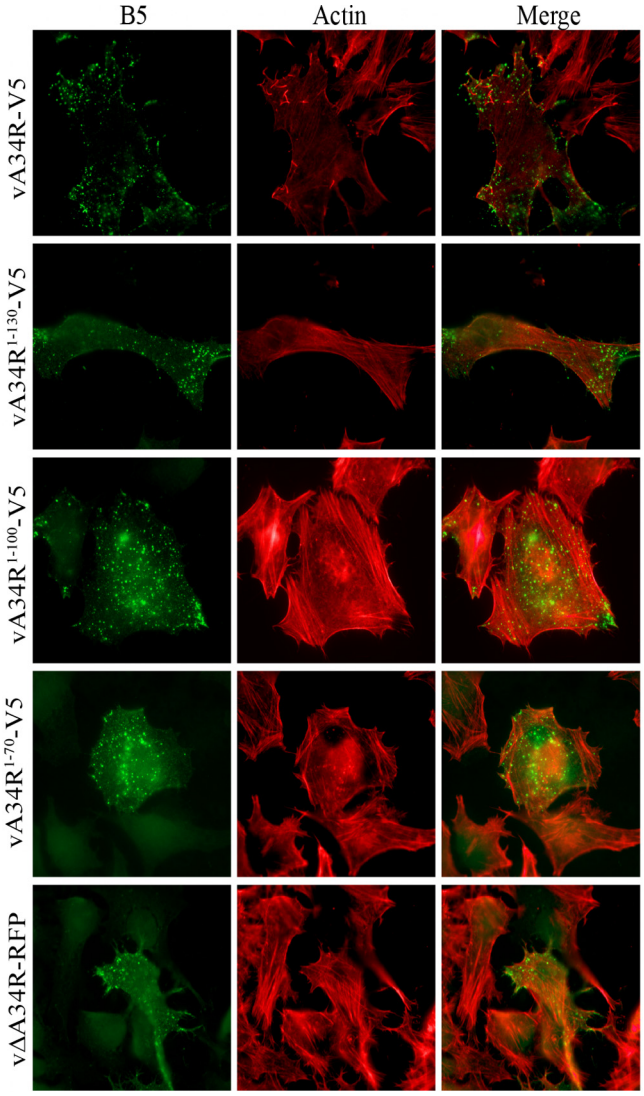

FIG 7 Actin tail formation. HeLa cells were grown on coverslips and infected with the indicated viruses at an MOI of 0.5. Cells were fixed at 8 hpi and stained with anti-B5 mAb followed by Cy2-conjugated anti-rat (green). Coverslips were subsequently permeabilized and incubated with Alexa Fluor 647-conjugated phalloidin to stain F-actin (red). Coverslips were mounted on microscope slides and visualized via fluorescence microscopy.

RFP than for a virus expressing the full coding sequence of A34R (vA34R-V5), as has been previously reported (33, 43), and for the A34 truncation viruses. Additionally, A34 was detected in EV lysates for each of the recombinants, apart from vA34R$^{1-100}$-V5, which is likely due to poor expression (Fig. 9B). However, there was less A34 detected for the truncations than for A34R-V5. We also determined the level of A33 incorporation into EV produced by our recombinant viruses. Similar to B5 results, less A33 was detected in EV lysates for each of our truncation viruses than for vA34R-V5, and slightly less A33 was detected in EV produced by ΔA34R-RFP than for the truncations (Fig. 9A). Importantly, the levels of IMV protein L1 were approximately equal for each of the recombinants, indicating that equal numbers of virions were assayed (Fig. 9A).

EV production is unaltered by the removal of the C-terminal residues of A34. Plaque size represents the ability of VACV to spread from cell to cell, which is directly related to the amount of infectious EV produced (14, 15, 20–22, 49, 50). To determine if the small-plaque phenotype exhibited by the A34 truncation viruses is due to a defect in EEV production, we measured the amount of EEV produced at 36 h postinfection

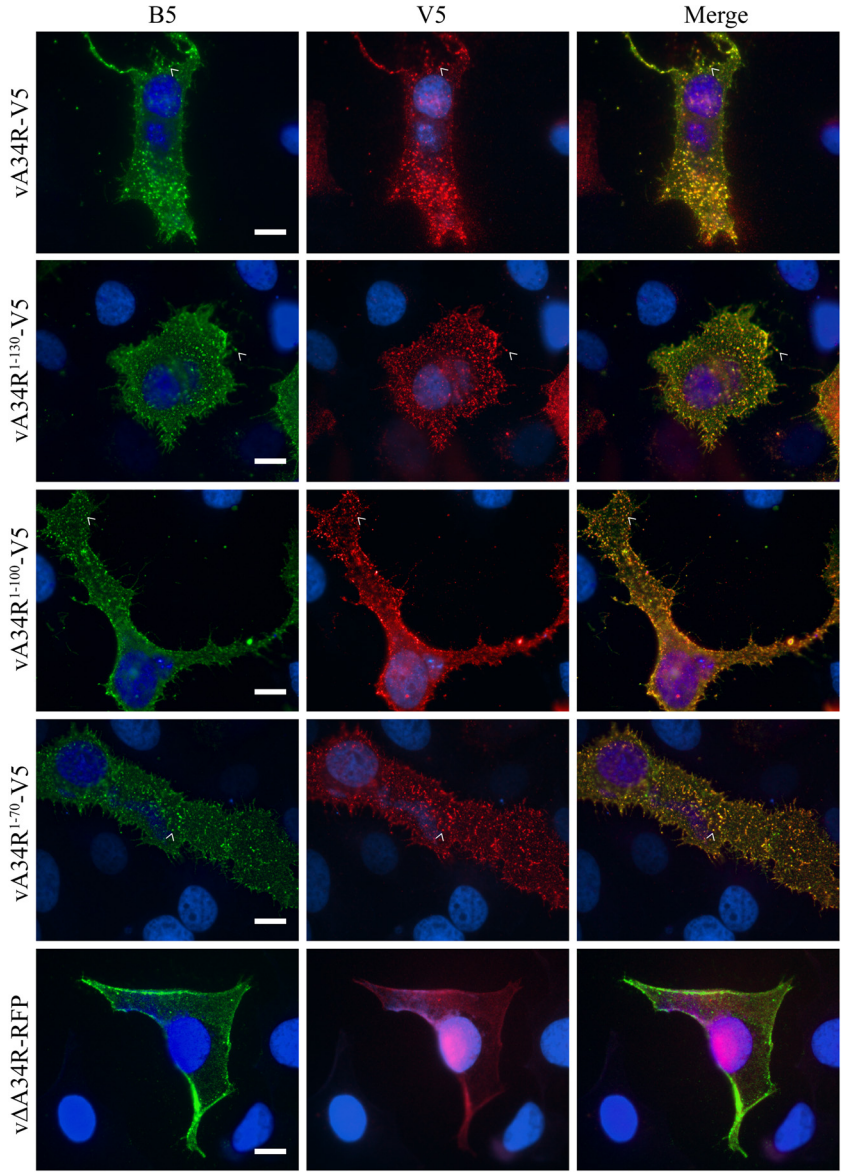

FIG 8 Cell surface staining of B5 and A34. HeLa cells were grown on coverslips and infected with the indicated viruses at an MOI of 0.5. The next day, cells were fixed on ice and stained with anti-B5 and anti-V5 mAbs, followed by Cy2-conjugated anti-rat (green) and Alexa Fluor 594-conjugated anti-mouse (red) antibodies. Coverslips were mounted on microscope slides with ProLong Gold antifade reagent with DAPI to stain DNA-containing particles (blue) and imaged via fluorescence microscopy. The overlap of B5 (green) and V5 (red) is shown in yellow. Red staining in the vΔA34R-RFP panel refers to RFP fluorescence and not V5 staining. Localization at VSPs is represented by arrowheads. Bars, 10 μm.

(hpi) (Fig. 10). RK13 cells were infected with vA34R-V5, vA34R$^{1-130}$-V5, vA34R$^{1-100}$-V5, vA34R$^{1-70}$-V5, and vΔA34R-RFP at a multiplicity of infection (MOI) of 5 for 36 h, and supernatants containing EEV or IMV were titrated by a plaque assay to measure total infectious virions. DNA was isolated, and quantitative real-time PCR (qPCR) was conducted to measure total genome copies per milliliter. Cells infected with vA34R$^{1-130}$-V5, vA34R$^{1-100}$-V5, and vA34R$^{1-70}$-V5 produced more infectious EEV than did cells infected with vA34R-V5 and vΔA34R-RFP, as determined by plaque assays. Total genome copy numbers and infectious virion production were increased in cells infected with recombinant viruses expressing A34 C-terminal truncations, approximately 0.5 to 1 log and 1.5 to 2 logs, respectively, for EEV compared to vA34R-V5 and vΔA34R-RFP (Fig. 10). Apart from vΔA34R-RFP and vA34R-V5, levels of IMV production were similar between

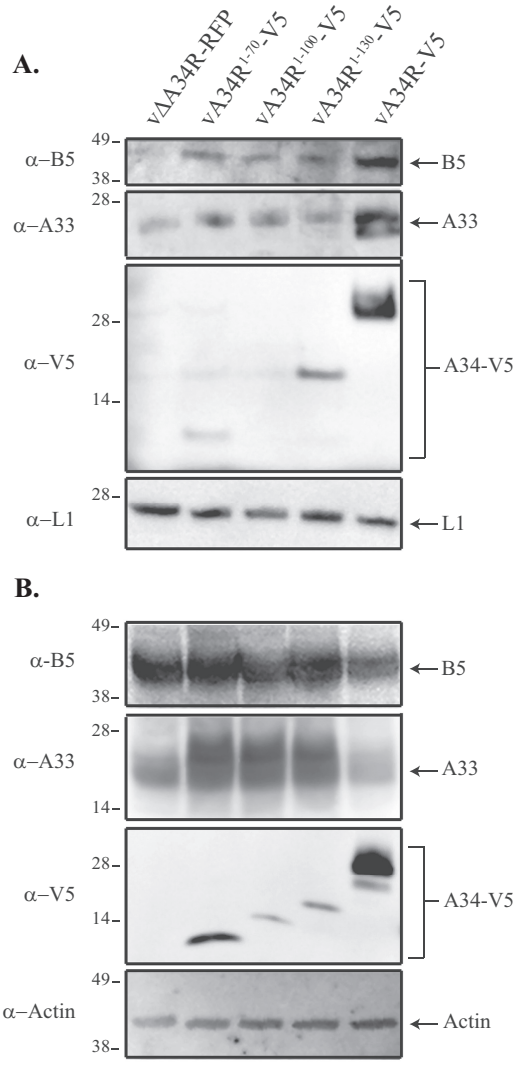

FIG 9 EV membrane protein composition. (A) RK13 cells were infected with the indicated viruses at an MOI of 5 and incubated at 37°C overnight. The next day, virions were isolated and analyzed by Western blotting with anti-B5, anti-V5, anti-A33 antiserum, and anti-L1 antiserum. (B) Infected cells were harvested, lysed in RIPA buffer, and analyzed by Western blotting with anti-B5, anti-V5, anti-A33 antiserum, and anti-actin. The positions and molecular weights in kilodaltons are shown on the left of the blots.

each of the truncation viruses, suggesting equal virus infection. Taken together, these results show that truncation of the C-terminal residues of A34 does not appreciably affect EEV production and suggest that a defect in EEV production does not explain the small-plaque phenotype exhibited by these recombinant viruses.

Deletion of the C-terminal residues of A34 reduces the ability of EEV to bind cells. Previous results show that the recombinant viruses with C-terminal truncations in A34 do not have a defect in EEV production (Fig. 10) but have a small-plaque phenotype (Fig. 4), suggesting a defect in either cell binding or entry. We therefore wanted to determine the ability of EEV produced by our recombinant viruses to bind cells. EEV produced from cells infected with the recombinant viruses was bound to BSC-40 cells on ice, and the numbers of viral DNA genomes bound to cells and in the inoculum were quantified by qPCR. EEV produced from cells infected with vΔA33R was used as a negative control, as it has previously been shown that these EEV bind inefficiently to cells (51). EEV from each of the recombinants, including vΔA34R-RFP, bound cells with similar efficiencies, which were

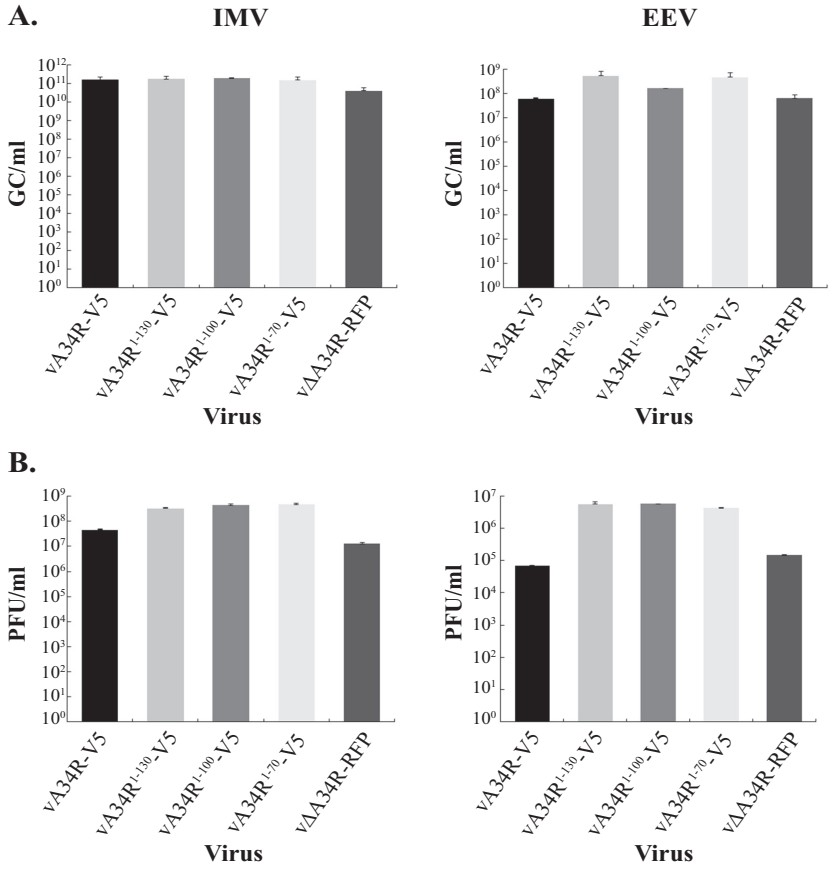

FIG 10 IMV and EEV production. Cells were infected at an MOI of 5 and incubated at 37°C. After 36 hpi, IMV (left) and EEV (right) were isolated, and total genome copies (GC) per milliliter were determined by qPCR (A) and titrated by a plaque assay to measure infectious virions (B). Error bars represent standard errors of the means (SEM).

approximately 50 to 70% lower than for vA34R-V5, but bound cells with a marginally higher efficiency than vΔA33R (Fig. 11). These data show that the C-terminal residues of A34 are important for cell binding.

The C-terminal residues of A34 are required for polyanion-induced nonfusogenic dissolution. Polyanion molecules, such as dextran sulfate (DS), have previously been shown to induce the nonfusogenic dissolution of the EEV membrane (52), which is required to expose the IMV-containing entry-fusion complex necessary for cell entry (53–56). The above-described results show a reduced ability of our recombinants to bind cells (Fig. 11). In addition, vΔA34R has been shown to be resistant to nonfusogenic dissolution (52). Therefore, we were interested in whether our recombinant viruses with C-terminal truncations in A34 also show resistance to DS-induced nonfusogenic dissolution. To test this, EEV were collected from cells infected with our recombinant viruses and subjected to an IMV-neutralizing antibody in either the presence or absence of DS. Importantly, when IMV produced by our recombinant viruses was subjected to IMV-neutralizing antibody, there was an approximately 25 to 50% reduction in titer, indicating that the IMV-neutralizing antibody was capable of IMV neutralization (data not shown). EEV produced by vA34R-V5 had an approximately 60% reduction in titer, while those produced by vΔA34R-RFP exhibited significant resistance to IMV neutralization, with approximately 93% of the titer remaining (Fig. 12). EEV produced by vA34R$^{1-130}$-V5, vA34R$^{1-100}$-V5, and vA34R$^{1-70}$-V5 showed a similar resistance to DS treatment compared to vΔA34R-RFP, retaining approximately 91%, 75%, and 83% of their titers, respectively. These results indicated that EEV membrane dissolution is

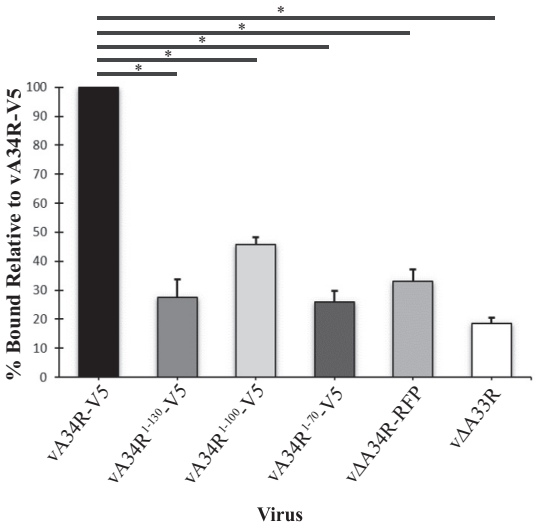

FIG 11 EEV cell binding. RK13 cells were infected with the indicated viruses at an MOI of 3 and incubated at 37°C. At 15 hpi, EEV were collected and tested for cell binding. Results are displayed as the percentage of genome copies bound to cells for each virus relative to the percentage of vA34R-V5 bound to cells. Error bars represent SEM. *, $P < 0.05$ by an unpaired *t* test.

impaired when the C-terminal residues of A34 are absent and suggest that these residues play a role in this process.

DISCUSSION

Interactions among EV proteins have been shown to be necessary to coordinate the localization and incorporation of these proteins into the wrapping membrane and

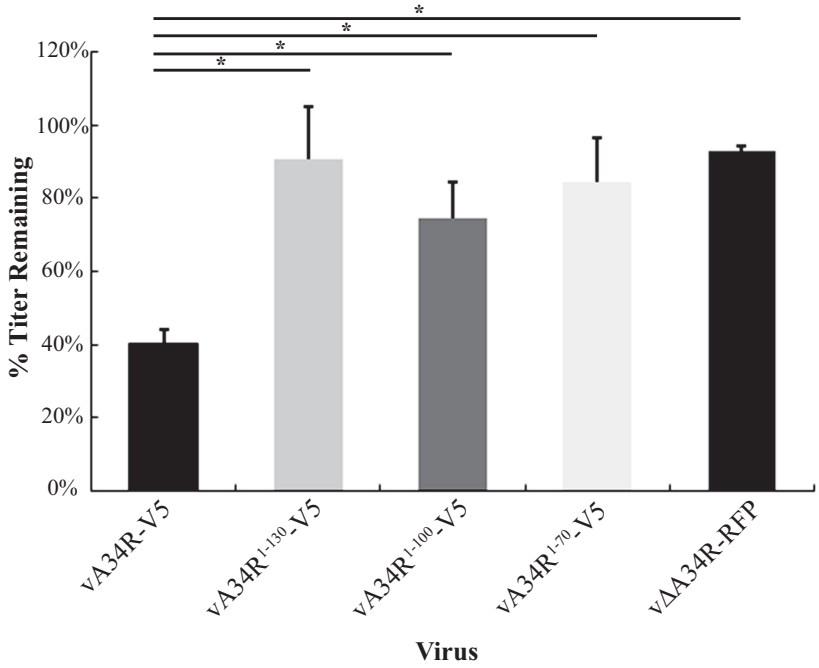

FIG 12 Polyanion-induced EEV membrane dissolution. BSC-40 cells were infected at 37°C with the indicated viruses. At 15 hpi, infected cell culture supernatants containing EEV were collected and clarified by low-speed centrifugation. Supernatants were diluted 1:5 in medium containing anti-L1 to neutralize IMV in the presence or absence of dextran sulfate and incubated for 1 h at 37°C. After incubation, treated samples were titrated on monolayers of BSC-40 cells at 37°C as described above. Results are shown as a percentage of the titer remaining compared to no polyanion treatment. Error bars represent SEM. *, $P < 0.05$ by an unpaired *t* test.

subsequently into the EV envelope, ensuring proper protein composition of the viral envelope (31–33, 35, 36, 43, 45, 51, 57, 58). Proper glycoprotein composition regulates the efficient production and release of infectious EV and is required for subsequent infections. The purposes of the present study were to determine the B5 interaction site on A34 as well as the role of this interaction for infectivity. Previous reports have shown that in cells infected with vΔA34R, B5 is both mislocalized and not incorporated into progeny virions (33, 43). Additionally, an interaction between A34 and B5, specifically between their ectodomains, has been described previously (43), and our data are consistent with this conclusion (Fig. 1). As a result, we hypothesized that the A34-B5 interaction was necessary for localization to the site of wrapping and for incorporation of B5 into released EV. C-terminal truncation constructs identified residues 1 to 80 of A34 as sufficient for interaction with B5 (Fig. 2E and F), and soluble ectodomain truncations of A34 suggested that A34 contains two regions (residues 57 to 100 and residues 100 to 168) that can independently interact with B5 (Fig. 3). This large B5 interaction site may in part explain why the charge-to-alanine (Fig. 2A and B) and small internal ectodomain (Fig. 2C and D) mutations were still capable of interacting with B5. While it seems likely that there is a single large region required for a high-affinity interaction with B5, having two separate binding sites on A34 would present the possibility that one molecule of A34 is capable of binding two molecules of B5 and that the two B5 binding sites on A34 have independent functions during protein trafficking, morphogenesis, and egress.

Having determined the B5 interaction site on A34, we constructed and characterized a set of recombinant VACVs expressing either a full, a partial, or no B5 interaction site based on the residues that we define above (Fig. 2 and 3). Previous reports suggesting a dependence of B5 on A34 for localization and wrapping (33, 43) led us to theorize that removing residues 80 to 130 of A34 would show a defect in infectious EV production similar to that of a full A34 deletion virus and that viruses expressing a partial or full B5 interaction site would have no or a minimal defect. Surprisingly, although our coimmunoprecipitation assay shows a strong, detectable interaction of A34 with B5 only for the virus expressing the full B5 interaction site (vA34R$^{1-130}$-V5) (Fig. 5), each recombinant virus showed a small-plaque phenotype similar to those of vΔA34R and vΔA34R-RFP (Fig. 4). These results suggest a defect in infectious EV production unrelated to a loss of the above-described B5-A34 interaction site. We also found it interesting that coimmunoprecipitation of cells infected with vA34$^{1-130}$-V5 precipitated more B5 than that of cells infected with vA34R-V5. An identical result was reported for certain charge-to-alanine mutations in A33 (58). The mutants also resulted in a small-plaque phenotype. Further analysis determined that as a result of this stronger interaction, A33 and B5 exist as a detectable complex on the surface of EV and resulted in a reduction in the ability of EV to bind cells (58). It has also been reported that A34 and B5 are present as a complex on the surface of EV during infection (46), and the addition of glycosaminoglycans (GAGs) resulted in a reduction in complex formation. If A34 and B5 exist as a complex on EV, then it is possible that the more durable interaction that we see in cells infected with vA34R$^{1-130}$-V5 causes a reduction in infectivity similar to that of the stronger A33-B5 interaction. We hypothesize that upon binding GAGs, the A34-B5 complex is induced to dissociate to allow for efficient cell binding, but a stronger A34-B5 interaction would inhibit this dissociation and cause a cell binding defect and a reduction in plaque size. However, as the defined B5 interaction site on A34 is truncated in vA34R$^{1-100}$-V5 and vA34R$^{1-70}$-V5, a reduction in cell binding could result from an absent A34-B5 complex on the surface of EV, which might be required for interaction with cell surface proteins such as GAGs. Taking these results into consideration, it is likely that the small-plaque phenotype attributed to our recombinants is the result of a combination of defects, some of which may differ between recombinants. Moreover, these results imply that the regulation of the A34-B5 interaction, especially as it pertains to cell binding, is critical during infection, and it will be of additional interest to further examine the A34-B5 complex on the surface of EV in these recombinants. Nonetheless, we cannot discount the possibility that the

C-terminal residues of A34, missing in each of our recombinants, contain a site necessary for cell binding and truncation of these residues and that removal of this site is directly responsible for the reduction in binding and the small-plaque phenotype. Additionally, A34 is known to be glycosylated, and its stability, localization, and glycosylation status have been reported to be affected by the presence or absence of B5 (17, 34, 45, 59). The glycosylation sites on A34 have not been reported. Therefore, we cannot discount the possibility that our truncations affect the glycosylation state of A34 and that this alone accounts for the phenotypes that we see.

Previous results suggested that the A34-B5 interaction is required for the localization of B5 to the site of wrapping and for incorporation into the EV envelope. However, B5 appeared to localize to the site of wrapping and in VSPs in cells infected with our recombinant viruses, even for the recombinant virus missing the defined B5 interaction site (Fig. 6). Additionally, the presence of B5- and A34-costained VSPs (Fig. 8) for each of our recombinants suggested that B5 is incorporated into the EV envelope, and further analysis of the EV membrane via Western blotting verified that both B5 and A34 are incorporated (Fig. 9) in each of the recombinants, even for the virus missing the B5 interaction site. These results suggested that the B5 interaction site that we have defined in this paper is not necessary for either localization or incorporation of B5. Importantly, we also observed that independent of whether residues 80 to 130 of A34 were present, similar amounts of A33 and B5 were detected in EV lysates, while noticeably smaller amounts were detected in the EV lysates of vΔA34R-RFP (Fig. 9). Taking these data into consideration, it seems likely that a transient B5 interaction site exists within the first 80 residues of A34 that accounts for the proper trafficking of B5 to the site of wrapping and for the increased B5 and A33 incorporation levels for the recombinants compared to vΔA34R-RFP, although it is also possible that A33, an EV protein that has also been shown to interact with B5, is compensating for the loss of the B5 interaction site on A34. For orthopoxviruses, several factors can contribute to a small-plaque phenotype, including a reduction in the number of EV produced, the ability to form actin tails, cell binding, and entry. Here we found that the recombinants were unable to produce actin tails (Fig. 7). As actin tail formation requires the incorporation and phosphorylation of A36 (60), a likely explanation is that the recombinants, all of which are missing the C-terminal residues of A34, cause an altered interaction with A36 either directly with A34 or indirectly via other EV proteins, such as A33 and B5. However, a complete abrogation in actin tail formation results in only an approximately 30% decrease in plaque size (47), suggesting that additional defects were present to account for the small-plaque phenotype. Indeed, further analysis shows that each of the recombinants, as well as vΔA34R-RFP, has a defect in the ability of EV to bind cells (Fig. 11) and in polyanion-induced nonfusogenic dissolution (Fig. 12). These results indicate that defects in actin tail formation, EV cell binding, and EV dissolution contribute to the small-plaque phenotype attributed to these recombinant viruses.

Although characterization of the vΔA34R virus has been conducted previously (42, 48), it is still not fully understood what causes the small-plaque phenotype. Studies of A34 have revealed that it is a multifunctional protein, with roles in determining EV protein content (33) (Fig. 9), retention of progeny CEV on the cell surface (41) (Fig. 7), and nonfusogenic dissolution of the outer EV envelope (52) (Fig. 12). A34 has also been suggested to have a role in EV binding to target cells (41), but direct evidence for this was lacking. Here, using a sensitive binding assay, we determined that deletion of the C-terminal residues of A34 significantly reduces the ability of EV to bind cells (Fig. 11), even when both A33 and B5 are present (Fig. 9). These results suggest that A34 plays a direct role in target cell binding. Importantly, residues 47 to 163 of the ectodomain of A34 have been shown to have homology to CTLDs (17). As CTLDs are implicated in ligand binding, homology to CTLDs implicates A34 in a role for cell binding. Proteins containing CTLDs make up a superfamily of extracellular proteins with diverse functions related by either structural fold or sequence similarity (61), and CTLD-containing proteins have been shown to bind a wide variety of ligands (62). Furthermore, a distinct subset of family members, including CD44, is capable of binding GAGs, like hyaluronan

(63–65). Additionally, our results provide an explanation for the small-plaque phenotype and loss of EV infectivity characteristic of the vΔA34R virus (42), which we have directly shown in this study to be a defect in cell binding (Fig. 11). A33 also contains a CTLD (66); thus, it is possible that the CTLDs within A33 and A34 cooperatively function for efficient cell binding. However, evidence for this is lacking. Alternatively, the defect in EV cell binding for our recombinant viruses could be indirectly due to the decrease in A33 and B5 incorporation (Fig. 9), as our laboratory has shown that both an A33 deletion virus (vΔA33R) and a B5 deletion virus (vΔB5R) exhibit a defect in the ability of EV to bind cells (51, 58). A33 and A34, both of which independently interact with B5, could indirectly form a complex on the surface of EV and mediate cooperative cell binding. Altogether, these results clearly suggest that glycoproteins A34, A33, and B5 have active roles in EV cell binding. It will be of interest to understand the extent of these proteins' participation in target cell binding, which may be a result of differential protein binding capabilities or due to the separate roles that these proteins play in glycoprotein incorporation.

Throughout our investigations, we noted several obvious differences in the characterization of vΔA34R-RFP compared to previous characterizations of vΔA34R. First, previous studies have described a 19- to 24-fold increase in the amount of EEV produced from cells infected with vΔA34R, with a reduction of 5- to 6-fold in infectivity compared with WR (42); however, our results utilizing vΔA34R-RFP show a similar amount of EEV produced compared to vA34R-V5 (Fig. 10), although the almost 1.5-log difference in IMV production for vΔA34R-RFP could explain these differences. Additionally, we noticed that a moderate amount of B5 localized to the site of wrapping in cells infected with vΔA34R-RFP, although this localization was less defined (Fig. 6), which contradicts previous reports suggesting that B5 does not make it to the site of wrapping in the absence of A34 (43). We can think of several possibilities for these differences. First, vΔA34R (17, 33, 42, 43, 48) still contains approximately 20% of the A34R coding sequence, including residues 1 to 17 of the cytoplasmic tail and residues 157 to 168 of the ectodomain, while vΔA34R-RFP removes the entire coding sequence of A34R, making it possible that the portion of A34R remaining in vΔA34R is responsible for these discrepancies. Furthermore, our laboratory has shown that in the absence of A33, B5 is properly localized to the site of wrapping and into progeny virions, but B5-GFP is not (51). It is possible that a similar mechanism occurs in the absence of A34, which would explain why Earley et al. reported mislocalization of B5-GFP in the absence of A34 (43). Moreover, a second B5 interaction site within the cytoplasmic region of A34, which would be present in our recombinant truncation viruses and vΔA34R, might properly localize B5 but not B5-GFP, providing an explanation for the discrepancies between this report and the report by Earley et al. Future studies should aim to better understand the discrepancies in EV production and B5 localization noted here between the previously described A34R deletion virus (vΔA34R) and the A34R deletion virus described here (vΔA34R-RFP).

MATERIALS AND METHODS

Cells. HeLa and BSC-40 cells were obtained from the ATCC and maintained in Dulbecco's modified Eagle's medium (DMEM) supplemented with 10% fetal bovine serum (FBS). RK13 cells were maintained in Eagle's minimum essential medium (EMEM) supplemented with 10% FBS.

Viruses. Recombinant viruses vTF7-3 and vΔA34R were described previously (43, 67). In order to construct recombinant viruses that have various amounts of the A34 C terminus deleted, a virus that has the entire A34R ORF replaced with a red fluorescent protein (vΔA34R-RFP) was created using homologous recombination. A DNA construct was synthesized (Integrated DNA Technologies) to replace the entire A34R ORF with the red fluorescent protein mKate2 (RFP) and contained 300 bp of sequence immediately upstream and downstream of the A34R open reading frame. HeLa cells were infected with WR and transfected with the synthesized construct to allow for recombination. A virus expressing red fluorescence was purified by 4 rounds of sequential plaque purification. The final recombinant was amplified, and the A34R locus was sequenced to ensure the replacement of A34R with RFP. Constructs containing 500 bp of sequence immediately upstream of the A34R ORF and encoding the first 70, 100, 130, or 168 residues of A34R followed by the coding sequence for the V5 epitope (underlined), a stop codon (bold), and a HindIII restriction site (italics) were generated by PCR using primer *CAAGCTTA*CGTAGAATCGAGACCGAGGAGAGGGTTAGGGATAGGCTTACCATTATCAGAAGACATTTTAATGTTAGTATCTAA, *CAA*

*GC**TTA***CGTAGAATCGAGACCGAGGAGAGGGTTAGGGATAGGCTTACCATCTTTATAAAAAATACTAAACAATAC TCTCAG, *CAAGC**TTA***CGTAGAATCGAGACCGAGGAGAGGGTTAGGGATAGGCTTACCTTTAAAATTTGTTAATTT ACTAATATCTATATCTTT, or *CAAGC**TTA***CGTAGAATCGAGACCGAGGAGAGGGTTAGGGATAGGCTTACCCTTA TAGAATTTTTTAACACATAGTACAGATTGAGT, respectively, in conjunction with the primer CCTCGAGACG CGTGATTGGTCTATG. The 500 bp of sequence immediately downstream of the A34R ORF was amplified using primers *CAAGCTT*CTACAAGTGACAACAAAAAATGAATTAATAATAA and GAATTCAGATTATCTGAAGG ATTGATGATTAGATGATAATCTCCAGCT. The resulting fragment has a HindIII restriction site (italics) at the 5′ end. The downstream sequence was appended to the truncation constructs using standard cloning methods. The resulting fragments were sequenced to confirm their integrity and used to create recombinant viruses expressing A34 with a V5 epitope tag (vA34R-V5) or one of the three truncations described above (vA34R$^{1-130}$-V5, vA34R$^{1-100}$-V5, or vA34R$^{1-70}$-V5) by homologous recombination with vΔA34R-RFP and the method described above. Recombinant viruses were isolated by picking plaques that did not express RFP. The A34R locus was sequenced in all the recombinants to verify their sequence.

Plasmid constructs. Plasmid pV5-A34 or pB5-GFP in pcDNA3.3 was described previously (43). Plasmid pA34-V5 was generated by PCR with primers that added the coding sequence for the V5 epitope tag immediately upstream of the stop codon of A34, and the resulting PCR product was subsequently transferred under the control of the T7 promoter into pcDNA3.3 (Invitrogen) using standard cloning techniques.

(i) Alanine mutants. Using pA34-V5 as the template, the coding sequence for charged residues 164, 165, and 168 (pA34$^{164-168A}$-V5); 118, 119, 120, 122, and 125 (pA34$^{118-125A}$-V5); 110, 111, and 114 (pA34$^{110-114A}$-V5); 84, 86, 88, and 91 (pA34^{84-91A}-V5); or 77, 79, and 81 (pA34^{77-81A}-V5) was mutated to encode alanine by two-step overlapping PCR. The charged residues from positions 76 to 91 (pA34^{76-91A}-V5) were mutated to alanine by two-step overlapping PCR with A34^{77-81A}-V5 as the template. These were then inserted under the control of the T7 promoter into pcDNA3.3 using standard cloning techniques.

(ii) Internal deletion mutants. Two-step PCR was performed using pV5-A34 as the template to delete the coding sequence of residues 40 to 55 (pV5-A34$^{\Delta 40-55}$), 57 to 77 (pV5-A34$^{\Delta 57-77}$), 78 to 89 (pV5-A34$^{\Delta 78-89}$), 92 to 109 (pV5-A34$^{\Delta 92-109}$), 111 to 124 (pV5-A34$^{\Delta 111-124}$), 125 to 144 (pV5-A34$^{\Delta 125-144}$), or 146 to 168 (pV5-A34$^{\Delta 146-168}$). pA34-V5 was used as the template to create pA34$^{\Delta 39-148}$-V5. The resulting PCR products were inserted into pcDNA3.3 using standard cloning techniques.

(iii) Truncation constructs. To create the C-terminal truncations in A34, an upstream primer that included the T7 promoter sequence was used with a downstream primer that inserted a stop codon immediately after amino acid 50 (pV5-A34$^{1-50}$), 60 (pV5-A34$^{1-60}$), 70 (pV5-A34$^{1-70}$), 80 (pV5-A34$^{1-80}$), 90 (pV5-A34$^{1-90}$), 100 (pV5-A34$^{1-100}$), 110 (pV5-A34$^{1-110}$), 120 (pV5-A34$^{1-120}$), 130 (pV5-A34$^{1-130}$), or 140 (pV5-A34$^{1-140}$) to amplify the desired region using pV5-A34 as the template. Amplified products were ligated into pcDNA3.3. The ectodomain of A34-V5 (pA34$^{36-168}$-V5) and segments thereof, including residues 57 to 168 (pA34$^{57-168}$-V5), 57 to 130 (pA34$^{57-130}$-V5), 57 to 100 (pA34$^{57-100}$-V5), 100 to 168 (pA34$^{100-168}$-V5), 100 to 130 (pA34$^{100-130}$-V5), or 130 to 168 (pA34$^{130-168}$-V5), were amplified by PCR using pA34-V5 as the template, an upstream primer that encoded the cleavable signal sequence of human serum albumin, and a downstream primer that added the coding sequence of the V5 epitope tag. These PCR products were cloned into the Topo TA cloning vector pCR2.1 (Invitrogen), sequenced, and subsequently cloned into the vector pcDNA3.3 under the control of the T7 promoter. All plasmid constructs were verified by sequencing.

Plaque assays and virus quantification. Confluent monolayers of BSC-40 cells were infected for 2 h, overlaid with DMEM containing 2.5% FBS and methylcellulose, and incubated at 37°C. After 3 days at 37°C, medium was removed, and cells were stained with crystal violet. For IMV and EEV production, monolayers of BSC-40 cells were infected for 2 h at an MOI of 5. After 2 h, cells were washed twice with phosphate-buffered saline (PBS) and overlaid with medium containing 2.5% FBS. At 36 h postinfection (hpi), EEV and IMV were isolated, as previously described (68). EEV samples were treated with 3 μg/ml of anti-L1 mAb (catalog number NR-45114; BEI Resources) for 1 h at 37°C to neutralize IMV before titration. EEV and IMV were titrated by a plaque assay on BSC-40 cell monolayers. Aliquots of each sample were treated with DNase I before encapsidated genomes were purified and analyzed by qPCR as previously described (68).

Immunoprecipitation. For plasmid transfections, HeLa cells were infected with vTF7-3 at an MOI of 5 and transfected at 2 hpi with the indicated constructs using Lipofectamine (Invitrogen) according to the manufacturer's instructions. Where stated, 40 μg/ml cytosine arabinoside (AraC; Sigma) was present throughout infection and transfection. For virus infections, HeLa cells were infected with the indicated viruses at an MOI of 5 and incubated overnight at 37°C. The following day, cells were harvested, lysed in radioimmunoprecipitation (RIPA) lysis buffer (0.5× PBS, 0.5% sodium deoxycholate, 1% Triton X-100, 1% NP-40, 0.1% sodium dodecyl sulfate, 0.2 mM phenylmethylsulfonyl fluoride, and a minicocktail protease inhibitor tablet [Roche]) on ice for 20 min, followed by centrifugation at 14,000 × *g* for 20 min at 4°C to clarify the supernatant. Immunoprecipitation was done using either protein G-agarose (Calbiochem) or protein G-Dynabeads (Invitrogen). For protein G-agarose, supernatants were precleared with protein G-agarose beads before incubation overnight with rat anti-B5 (mAb 19C2) (9). Immunocomplexes were incubated with protein G-agarose beads for 2 h at 4°C, washed three times with lysis buffer, resuspended in protein loading buffer, and resolved by polyacrylamide gel electrophoresis (PAGE), followed by transfer to nitrocellulose. Proteins were visualized by immunoblot analysis using horseradish peroxidase (HRP)-conjugated mouse anti-V5 mAb (Invitrogen), mouse anti-V5 mAb (Invitrogen) followed by anti-mouse HRP (Jackson), mouse anti-GFP mAb (Abcam) followed by anti-mouse HRP, or rat anti-B5 mAb followed by anti-rat HRP (Jackson) and developed with chemiluminescence reagents (Pierce)

according to the manufacturer's instructions. For protein G-Dynabeads, supernatants were incubated with protein G-magnetic Dynabeads complexed to either mouse anti-V5 mAb or rat anti-B5 mAb for 1 h at 4°C, washed three times with lysis buffer, and resuspended in protein gel sample buffer. Samples were resolved by PAGE, followed by transfer to nitrocellulose. Proteins were visualized by immunoblot analysis using mouse anti-V5 mAb followed by anti-mouse HRP, rat anti-B5 mAb followed by anti-rat Alexa Fluor 647 (Jackson), rabbit anti-B5 antiserum (NR-629; BEI Resources) followed by anti-rabbit HRP (Jackson), and mouse antiactin mAb (Invitrogen) followed by anti-mouse Alexa Fluor 750 (Invitrogen). Membranes were developed with chemiluminescence reagents (Pierce) according to the manufacturer's directions, and both fluorescence and chemiluminescence signals were detected using a Kodak 4000MM Pro image station.

Immunofluorescence. HeLa cells grown on coverslips were infected with the indicated viruses at an MOI of 0.5. For intracellular staining, the following day, infected cells were fixed with 4% paraformaldehyde for 10 min and permeabilized with 0.1% Triton-X for 10 min. Following permeabilization, cells were incubated for 1 h at room temperature in PBS with rat anti-B5 mAb and mouse anti-V5 mAb followed by anti-rat Cy2-conjugated antibody (Jackson) and anti-mouse Alexa Fluor 594 (Jackson), respectively. For surface staining, the following day, cells were fixed and incubated with rat anti-B5 mAb and mouse anti-V5 mAb for 1 h on ice, followed by incubation with anti-rat Cy2 and anti-mouse Alexa Fluor 594. To assay actin tail formation, cells were incubated for 1 h at room temperature in PBS with rat anti-B5 mAb followed by anti-rat Cy2-conjugated antibody and then permeabilized in 0.1% Triton X-100 for 10 min and incubated with Alexa Fluor 647-conjugated phalloidin (Invitrogen) for 20 min. Coverslips were mounted using ProLong Gold antifade reagent with 4′,6-diamidino-2-phenylindole (DAPI; Life Technologies). Cells were imaged using a Leica DMIRB inverted fluorescence microscope with a cooled charge-coupled device (Cooke) controlled by Image-Pro Plus software (Media Cybernetics). Images were compiled and minimally processed using Photoshop (Adobe).

Virion incorporation. RK13 cells were infected with the indicated viruses at an MOI of 5. The next day, infected cell culture supernatants were collected and centrifuged at 913 × *g* to pellet cellular debris. Clarified supernatants containing EEV were layered on a 36% sucrose cushion and centrifuged at 100,000 × *g* for 10 min to pellet virions. Virus pellets were resuspended in 10 mM Tris (pH 9.0), diluted in protein gel sample buffer, and analyzed by Western blotting as described above. Proteins were visualized by immunoblot analysis using rat anti-B5 mAb followed by anti-rat HRP, mouse anti-V5 mAb followed by anti-mouse HRP, rabbit anti-A33 antiserum (catalog number NR-628; BEI Resources) followed by anti-rabbit HRP (Pierce), rabbit anti-L1 antiserum (NR-631; BEI Resources) followed by anti-rabbit HRP, and anti-mouse actin mAb followed by anti-mouse Alexa Fluor 750. Membranes were developed with chemiluminescence reagents (Pierce) according to the manufacturer's directions, and fluorescence and chemiluminescence signals were detected using a Kodak 4000MM Pro image station.

Cell binding. A virus binding assay was performed essentially as previously described (68, 69). RK13 cells were infected with the indicated viruses at an MOI of 3. At 15 hpi, infected cell culture supernatants were collected and clarified by centrifugation at 913 × *g* for 10 min. Aliquots of each sample were treated with DNase I before encapsidated genomes were purified and analyzed by qPCR. Monolayers of BSC-40 cells were treated with PBS containing 0.6 mM EDTA for 15 min at 37°C to detach cells, and 1×10^5 cells were suspended in the infected cell culture supernatant and rotated at 4°C for 1 h. After binding, cells were pelleted, and viral DNA was quantified by qPCR.

Polyanion-induced membrane dissolution. A plaque reduction assay was performed essentially as previously described (52, 69). BSC-40 cells were infected with the indicated viruses at an MOI of 5 and incubated at 37°C. At 15 hpi, infected cell supernatants were collected and clarified at 913 × *g* for 10 min. Supernatants were transferred to fresh tubes, diluted 1:5, and treated with 3 μg/ml anti-L1 mAb (NR-45114; BEI Resources) in the presence or absence of 2 μg/ml high-molecular-weight dextran sulfate (M_r of >500,000; Sigma) for 1 h at 37°C. Titers were determined by a plaque assay, as described above.

ACKNOWLEDGMENTS

We thank Bernard Moss for providing vΔA34R. The following reagents were obtained through BEI Resources, NIAID, NIH: monoclonal anti-vaccinia virus (WR) L1R protein, residues 1 to 185 (similar to VMC-2) (produced *in vitro*) (NR-45114); polyclonal anti-vaccinia virus (WR) L1R protein (antiserum, rabbit) (NR-631); polyclonal anti-vaccinia virus (WR) A33R protein (antiserum, rabbit) (NR-628); and polyclonal anti-vaccinia virus (WR) B5R protein (antiserum, rabbit) (NR-629).

This work was supported in part by NIH grants AI067391 and AI117105. S.R.M. was supported by award number T32AI118689 from the National Institute of Allergy and Infectious Diseases.

REFERENCES

1. Moss B. 2013. Poxvirus DNA replication. Cold Spring Harb Perspect Biol 5:a010199. https://doi.org/10.1101/cshperspect.a010199.
2. Yang Z, Bruno DP, Martens CA, Porcella SF, Moss B. 2010. Simultaneous high-resolution analysis of vaccinia virus and host cell transcriptomes by deep RNA sequencing. Proc Natl Acad Sci U S A 107:11513–11518. https://doi.org/10.1073/pnas.1006594107.
3. Moss B. 2001. Poxviridae: the viruses and their replication, p 2849–2883. *In* Knipe DM, Howley PM, Griffin DE, Lamb RA, Martin MA, Roizman B,

Straus SE (ed), Fields virology, 4th ed. Lippincott Williams & Wilkins, Philadelphia, PA.
4. Appleyard G, Hapel AJ, Boulter EA. 1971. An antigenic difference between intracellular and extracellular rabbitpox virus. J Gen Virol 13:9–17. https://doi.org/10.1099/0022-1317-13-1-9.
5. Hollinshead M, Vanderplasschen A, Smith GL, Vaux DJ. 1999. Vaccinia virus intracellular mature virions contain only one lipid membrane. J Virol 73:1503–1517.
6. Grimley PM, Rosenblum EN, Mims SJ, Moss B. 1970. Interruption by rifampin of an early stage in vaccinia virus morphogenesis: accumulation of membranes which are precursors of virus envelopes. J Virol 6:519–533.
7. Sanderson CM, Hollinshead M, Smith GL. 2000. The vaccinia virus A27L protein is needed for the microtubule-dependent transport of intracellular mature virus particles. J Gen Virol 81:47–58. https://doi.org/10.1099/0022-1317-81-1-47.
8. Ploubidou A, Moreau V, Ashman K, Reckmann I, González C, Way M. 2000. Vaccinia virus infection disrupts microtubule organization and centrosome function. EMBO J 19:3932–3944. https://doi.org/10.1093/emboj/19.15.3932.
9. Schmelz M, Sodeik B, Ericsson M, Wolffe EJ, Shida H, Hiller G, Griffiths G. 1994. Assembly of vaccinia virus: the second wrapping cisterna is derived from the *trans* Golgi network. J Virol 68:130–147.
10. Sivan G, Weisberg AS, Americo JL, Moss B. 2016. Retrograde transport from early endosomes to the *trans*-Golgi network enables membrane wrapping and egress of vaccinia virus virions. J Virol 90:8891–8905. https://doi.org/10.1128/JVI.01114-16.
11. Ward BM, Moss B. 2001. Visualization of intracellular movement of vaccinia virus virions containing a green fluorescent protein-B5R membrane protein chimera. J Virol 75:4802–4813. https://doi.org/10.1128/JVI.75.10.4802-4813.2001.
12. Hollinshead M, Rodger G, Van Eijl H, Law M, Hollinshead R, Vaux DJ, Smith GL. 2001. Vaccinia virus utilizes microtubules for movement to the cell surface. J Cell Biol 154:389–402. https://doi.org/10.1083/jcb.200104124.
13. Blasco R, Moss B. 1992. Role of cell-associated enveloped vaccinia virus in cell-to-cell spread. J Virol 66:4170–4179.
14. Payne LG. 1980. Significance of extracellular enveloped virus in the in vitro and in vivo dissemination of vaccinia. J Gen Virol 50:89–100. https://doi.org/10.1099/0022-1317-50-1-89.
15. Smith GL, Vanderplasschen A, Law M. 2002. The formation and function of extracellular enveloped vaccinia virus. J Gen Virol 83:2915–2931. https://doi.org/10.1099/0022-1317-83-12-2915.
16. Roper RL, Payne LG, Moss B. 1996. Extracellular vaccinia virus envelope glycoprotein encoded by the A33R gene. J Virol 70:3753–3762.
17. Duncan SA, Smith GL. 1992. Identification and characterization of an extracellular envelope glycoprotein affecting vaccinia virus egress. J Virol 66:1610–1621.
18. van Eijl H, Hollinshead M, Smith GL. 2000. The vaccinia virus A36R protein is a type Ib membrane protein present on intracellular but not extracellular enveloped virus particles. Virology 271:26–36. https://doi.org/10.1006/viro.2000.0260.
19. Shida H. 1986. Nucleotide sequence of the vaccinia virus hemagglutinin gene. Virology 150:451–462. https://doi.org/10.1016/0042-6822(86)90309-0.
20. Wolffe EJ, Isaacs SN, Moss B. 1993. Deletion of the vaccinia virus B5R gene encoding a 42-kilodalton membrane glycoprotein inhibits extracellular virus envelope formation and dissemination. J Virol 67:4732–4741.
21. Zhang WH, Wilcock D, Smith GL. 2000. Vaccinia virus F12L protein is required for actin tail formation, normal plaque size, and virulence. J Virol 74:11654–11662. https://doi.org/10.1128/JVI.74.24.11654-11662.2000.
22. Blasco R, Moss B. 1991. Extracellular vaccinia virus formation and cell-to-cell virus transmission are prevented by deletion of the gene encoding the 37,000-dalton outer envelope protein. J Virol 65:5910–5920.
23. Zhou J, Sun XY, Fernando GJP, Frazer IH. 1992. The vaccinia virus K2L gene encodes a serine protease inhibitor which inhibits cell-cell fusion. Virology 189:678–686. https://doi.org/10.1016/0042-6822(92)90591-C.
24. Domi A, Weisberg AS, Moss B. 2008. Vaccinia virus E2L null mutants exhibit a major reduction in extracellular virion formation and virus spread. J Virol 82:4215–4226. https://doi.org/10.1128/JVI.00037-08.
25. van Eijl H, Hollinshead M, Rodger G, Zhang WH, Smith GL. 2002. The vaccinia virus F12L protein is associated with intracellular enveloped virus particles and is required for their egress to the cell surface. J Gen Virol 83:195–207. https://doi.org/10.1099/0022-1317-83-1-195.
26. Isaacs SN, Wolffe EJ, Payne LG, Moss B. 1992. Characterization of a vaccinia virus-encoded 42-kilodalton class I membrane glycoprotein component of the extracellular virus envelope. J Virol 66:7217–7224.
27. Turner PC, Moyer RW. 1995. Orthopoxvirus fusion inhibitor glycoprotein SPI-3 (open reading frame K2L) contains motifs characteristic of serine proteinase inhibitors that are not required for control of cell fusion. J Virol 69:5978–5987.
28. Dehaven BC, Gupta K, Isaacs SN. 2011. The vaccinia virus A56 protein: a multifunctional transmembrane glycoprotein that anchors two secreted viral proteins. J Gen Virol 92:1971–1980. https://doi.org/10.1099/vir.0.030460-0.
29. Schmutz C, Rindisbacher L, Galmiche MC, Wittek R. 1995. Biochemical analysis of the major vaccinia virus envelope antigen. Virology 213:19–27. https://doi.org/10.1006/viro.1995.1542.
30. Chan WM, Ward BM. 2012. The A33-dependent incorporation of B5 into extracellular enveloped vaccinia virions is mediated through an interaction between their lumenal domains. J Virol 86:8210–8220. https://doi.org/10.1128/JVI.00249-12.
31. Perdiguero B, Blasco R. 2006. Interaction between vaccinia virus extracellular virus envelope A33 and B5 glycoproteins. J Virol 80:8763–8777. https://doi.org/10.1128/JVI.00598-06.
32. Rottger S, Frischknecht F, Reckmann I, Smith GL, Way M. 1999. Interactions between vaccinia virus IEV membrane proteins and their roles in IEV assembly and actin tail formation. J Virol 73:2863–2875.
33. Perdiguero B, Lorenzo MM, Blasco R. 2008. Vaccinia virus A34 glycoprotein determines the protein composition of the extracellular virus envelope. J Virol 82:2150–2160. https://doi.org/10.1128/JVI.01969-07.
34. Payne LG. 1992. Characterization of vaccinia virus glycoproteins by monoclonal antibody precipitation. Virology 187:251–260. https://doi.org/10.1016/0042-6822(92)90313-E.
35. Dodding MP, Newsome TP, Collinson LM, Edwards C, Way M. 2009. An E2-F12 complex is required for intracellular enveloped virus morphogenesis during vaccinia infection. Cell Microbiol 11:808–824. https://doi.org/10.1111/j.1462-5822.2009.01296.x.
36. Johnston SC, Ward BM. 2009. Vaccinia virus protein F12 associates with intracellular enveloped virions through an interaction with A36. J Virol 83:1708–1717. https://doi.org/10.1128/JVI.01364-08.
37. Turner PC, Moyer RW. 2006. The cowpox virus fusion regulator proteins SPI-3 and hemagglutinin interact in infected and uninfected cells. Virology 347:88–99. https://doi.org/10.1016/j.virol.2005.11.012.
38. Engelstad M, Smith GL. 1993. The vaccinia virus 42-kDa envelope protein is required for the envelopment and egress of extracellular virus and for virus virulence. Virology 194:627–637. https://doi.org/10.1006/viro.1993.1302.
39. Lorenzo MM, Herrera E, Blasco R, Isaacs SN. 1998. Functional analysis of vaccinia virus B5R protein: role of the cytoplasmic tail. Virology 252:450–457. https://doi.org/10.1006/viro.1998.9483.
40. Mathew E, Sanderson CM, Hollinshead M, Smith GL. 1998. The extracellular domain of vaccinia virus protein B5R affects plaque phenotype, extracellular enveloped virus release, and intracellular actin tail formation. J Virol 72:2429–2438.
41. Blasco R, Sisler JR, Moss B. 1993. Dissociation of progeny vaccinia virus from the cell membrane is regulated by a viral envelope glycoprotein: effect of a point mutation in the lectin homology domain of the A34R gene. J Virol 67:3319–3325.
42. McIntosh AA, Smith GL. 1996. Vaccinia virus glycoprotein A34R is required for infectivity of extracellular enveloped virus. J Virol 70:272–281.
43. Earley AK, Chan WM, Ward BM. 2008. The vaccinia virus B5 protein requires A34 for efficient intracellular trafficking from the endoplasmic reticulum to the site of wrapping and incorporation into progeny virions. J Virol 82:2161–2169. https://doi.org/10.1128/JVI.01971-07.
44. Breiman A, Carpentier DCJ, Ewles HA, Smith GL. 2013. Transport and stability of the vaccinia virus A34 protein is affected by the A33 protein. J Gen Virol 94:720–725. https://doi.org/10.1099/vir.0.049486-0.
45. Breiman A, Smith GL. 2010. Vaccinia virus B5 protein affects the glycosylation, localization and stability of the A34 protein. J Gen Virol 91:1823–1827. https://doi.org/10.1099/vir.0.020677-0.
46. Roberts KL, Breiman A, Carter GC, Ewles HA, Hollinshead M, Law M, Smith GL. 2009. Acidic residues in the membrane-proximal stalk region of vaccinia virus protein B5 are required for glycosaminoglycan-mediated disruption of the extracellular enveloped virus outer membrane. J Gen Virol 90:1582–1591. https://doi.org/10.1099/vir.0.009092-0.

47. Ward BM, Moss B. 2001. Vaccinia virus intracellular movement is associated with microtubules and independent of actin tails. J Virol 75:11651–11663. https://doi.org/10.1128/JVI.75.23.11651-11663.2001.
48. Wolffe EJ, Katz E, Weisberg A, Moss B. 1997. The A34R glycoprotein gene is required for induction of specialized actin-containing microvilli and efficient cell-to-cell transmission of vaccinia virus. J Virol 71:3904–3915.
49. Roper RL, Wolffe EJ, Weisberg A, Moss B. 1998. The envelope protein encoded by the A33R gene is required for formation of actin-containing microvilli and efficient cell-to-cell spread of vaccinia virus. J Virol 72:4192–4204.
50. Wolffe EJ, Weisberg AS, Moss B. 1998. Role for the vaccinia virus A36R outer envelope protein in the formation of virus-tipped actin-containing microvilli and cell-to-cell virus spread. Virology 244:20–26. https://doi.org/10.1006/viro.1998.9103.
51. Chan WM, Ward BM. 2010. There is an A33-dependent mechanism for the incorporation of B5-GFP into vaccinia virus extracellular enveloped virions. Virology 402:83–93. https://doi.org/10.1016/j.virol.2010.03.017.
52. Law M, Carter GC, Roberts KL, Hollinshead M, Smith GL. 2006. Ligand-induced and nonfusogenic dissolution of a viral membrane. Proc Natl Acad Sci U S A 103:5989–5994. https://doi.org/10.1073/pnas.0601025103.
53. Senkevich TG, Ojeda S, Townsley A, Nelson GE, Moss B. 2005. Poxvirus multiprotein entry-fusion complex. Proc Natl Acad Sci U S A 102:18572–18577. https://doi.org/10.1073/pnas.0509239102.
54. Senkevich TG, Moss B. 2005. Vaccinia virus H2 protein is an essential component of a complex involved in virus entry and cell-cell fusion. J Virol 79:4744–4754. https://doi.org/10.1128/JVI.79.8.4744-4754.2005.
55. Townsley AC, Senkevich TG, Moss B. 2005. Vaccinia virus A21 virion membrane protein is required for cell entry and fusion. J Virol 79:9458–9469. https://doi.org/10.1128/JVI.79.15.9458-9469.2005.
56. Townsley AC, Senkevich TG, Moss B. 2005. The product of the vaccinia virus L5R gene is a fourth membrane protein encoded by all poxviruses that is required for cell entry and cell-cell fusion. J Virol 79:10988–10998. https://doi.org/10.1128/JVI.79.17.10988-10998.2005.
57. Wolffe EJ, Weisberg AS, Moss B. 2001. The vaccinia virus A33R protein provides a chaperone function for viral membrane localization and tyrosine phosphorylation of the A36R protein. J Virol 75:303–310. https://doi.org/10.1128/JVI.75.1.303-310.2001.
58. Chan WM, Ward BM. 2012. Increased interaction between vaccinia virus proteins A33 and B5 is detrimental to infectious extracellular enveloped virion production. J Virol 86:8232–8244. https://doi.org/10.1128/JVI.00253-12.
59. Payne L. 1978. Polypeptide composition of extracellular enveloped vaccinia virus. J Virol 27:28–37.
60. Frischknecht F, Moreau V, Rottger S, Gonfloni S, Reckmann I, Superti-Furga G, Way M. 1999. Actin-based motility of vaccinia virus mimics receptor tyrosine kinase signalling. Nature 401:926–929. https://doi.org/10.1038/44860.
61. Zelensky AN, Gready JE. 2005. The C-type lectin-like domain superfamily. FEBS J 272:6179–6217. https://doi.org/10.1111/j.1742-4658.2005.05031.x.
62. Drickamer K. 1999. C-type lectin-like domains. Curr Opin Struct Biol 9:585–590. https://doi.org/10.1016/S0959-440X(99)00009-3.
63. Kohda D, Morton CJ, Parkar AA, Hatanaka H, Inagaki FM, Campbell ID, Day AJ. 1996. Solution structure of the link module: a hyaluronan-binding domain involved in extracellular matrix stability and cell migration. Cell 86:767–775. https://doi.org/10.1016/S0092-8674(00)80151-8.
64. Aruffo A, Stamenkovic I, Melnick M, Underhill CB, Seed B. 1990. CD44 is the principal cell surface receptor for hyaluronate. Cell 61:1303–1313. https://doi.org/10.1016/0092-8674(90)90694-A.
65. Culty M, Miyake K, Kincade PW, Sikorski E, Butcher EC, Underhill C, Silorski E. 1990. The hyaluronate receptor is a member of the CD44 (H-CAM) family of cell surface glycoproteins. J Cell Biol 111:2765–2774. https://doi.org/10.1083/jcb.111.6.2765.
66. Su HP, Singh K, Gittis AG, Garboczi DN. 2010. The structure of the poxvirus A33 protein reveals a dimer of unique C-type lectin-like domains. J Virol 84:2502–2510. https://doi.org/10.1128/JVI.02247-09.
67. Fuerst TR, Niles EG, Studier FW, Moss B. 1986. Eukaryotic transient-expression system based on recombinant vaccinia virus that synthesizes bacteriophage T7 RNA polymerase. Proc Natl Acad Sci U S A 83:8122–8126. https://doi.org/10.1073/pnas.83.21.8122.
68. Baker JL, Ward BM. 2014. Development and comparison of a quantitative TaqMan-MGB real-time PCR assay to three other methods of quantifying vaccinia virions. J Virol Methods 196:126–132. https://doi.org/10.1016/j.jviromet.2013.10.026.
69. Bryk P, Brewer MG, Ward BM. 14 May 2018. Vaccinia virus phospholipase protein F13 promotes the rapid entry of extracellular virions into cells. J Virol https://doi.org/10.1128/JVI.02154-17.